2017 International Nuclear Atlantic Conference - INAC 2017
Belo Horizonte, MG, Brazil, October 22-27, 2017
ASSOCIAÇÃO BRASILEIRA DE ENERGIA NUCLEAR – ABEN

Agência Brasileira do ISBN
ISBN 978-85-99141-07-6
9 788599 141076

STUDY OF ABLATION ON SURFACES OF NUCLEAR-USE METALS IRRADIATED WITH FEMTOSECOND LASER

Alessandro F. Nogueira[1], Ricardo E. Samad[2], Nilson D. Vieira Jr.[2] and Wagner de Rossi[2]

[1] Centro Tecnológico da Marinha em São Paulo (CTMSP) and Faculdade de Engenharia de Sorocaba (FACENS)
Estrada Iperó-Sorocaba km 12,5
18560-000 Iperó, SP
alessandro.nogueira@usp.br

[2] Instituto de Pesquisas Energéticas e Nucleares (IPEN / CNEN - SP)
Av. Professor Lineu Prestes 2242
05508-000 São Paulo, SP
resamad@ipen.br

ABSTRACT

The use of ultrashort pulsed lasers is an alternative for micro-machining in metal surfaces, with diverse applications in several industrial areas, such as aeronautics, aerospace, naval, nuclear, among others, where there is a growing concern with reliability in service. In this work, micro-machining were performed on titanium surfaces using femtosecond ultrashort pulses. Such a process resulted in minimal heat transfer to the material, thus avoiding and surface deformation of the titanium plate and the formation of resolidified material in the ablated region, which are drawbacks present in the use of the long pulsed keyed laser of the order of nanoseconds. Three types of micro-machining were performed, with variations in the distances between the machined lines. It was also verified that the wettability increases when there is an increase in the distance between machined lines. Finally, in order to change the surface with minimal removal of material, it has been found that the use of ultra-short pulse lasers provide great benefits for the integrity of the ablated material. This initial study is the starting point for the study of other metals, such as Maraging Steels and Zircaloy that will be the target of future work.

1. INTRODUCTION

Micro-machining, which had previously only been researched in the scientific field, currently has applications in several industrial segments, such as aerospace and aeronautics, medical equipment, microelectronics and automotive, as well as micromotors, microfluidic circuits and microsystems [1]. Titanium alloys are widely used in embedded structural elements, so laser micro-alloying is an important alternative for the alteration of surface characteristics such as wettability, adhesion and color [2]. Since titanium is a specific high strength material, small thickness plates are used as parts of structural elements, so it is of the utmost importance that the micro-machining processes are controlled and do not cause damage to the material.

An important factor influencing precision in laser micro-machining is the thermally affected zone (ZTA), which extends beyond the region of laser pulse interaction and is responsible for a phase transformation by altering the properties of the material collaterally. The thermodynamic side effect is intrinsic to the ablation process when pulses longer than approximately 1 picosecond are used, this being the case of common lasers, which have a temporal width of the order of tens of nanoseconds. However, this factor can be minimized

by rapidly depositing energy through short and ultra-short pulses, thus ablating the material before heat diffusion occurs and affects the neighborhood of the interaction region [2,3].
One of the main characteristics of these pulses, when used for micro-machining, is the small ZTA, due to the particular dynamics of absorption and ablation generated by these ultra-short and ultra-intense pulses. The process of interaction of radiation with matter involves many phenomena that occur at different time scales, from femtoseconds to nanoseconds [4]. Ultrashort pulses of the order of femtoseconds allowed a deterministic interaction with a well-defined ablation threshold, but the ablation threshold does not depend only on the characteristics of the laser pulse and the type of ablated material. The absorption of the pulse also depends on the presence of defects in the crystalline structure of these materials. Pre-irradiation by a laser pulse in a material, even below the damage threshold, can create defects in the crystal lattice. This process is called the incubation effect and is responsible for decreasing the damage threshold in pre-irradiated materials. In this way, laser pulses that reach the pre-irradiated material have a greater facility in the ablation sequence of the material [5].
The surface micro-machining process requires the overlapping of pulses so that the required amount of material is removed. Thus, the ablation threshold and the incubation parameter are important parameters for the micro-machining and must be previously known. In this context, this work had its focus in the accomplishment of experiments imposing changes in the variables fluency, repetition rate and incubation parameters by the overlap of pulses.
To obtain the minimum heat transfer condition for the material, suitable process parameters need to be used. Thus, the fluency should be above the ablation threshold for the material. Therefore, the beginning of the work focused on obtaining low and high fluency regimes, and then micro-machining with process parameters appropriate to the material. For the measurement of the ablation threshold and the incubation parameter, the experimental technique Diagonal Scan (D-Scan) was used, and this technique was introduced by the IPEN Lasers and Applications Center, presented in [6].
The D-Scan technique is a simple method alternative to measure ultra-short pulse ablation threshold, consisting of traversing a sample longitudinally and transversely in the z and y directions, as shown in Fig. 1 (a), through the waist of the focused beam, to from a position before the waist. Thus, as shown in Fig. 1 (b) a symmetrical profile with two lobes is etched on the surface of the sample.

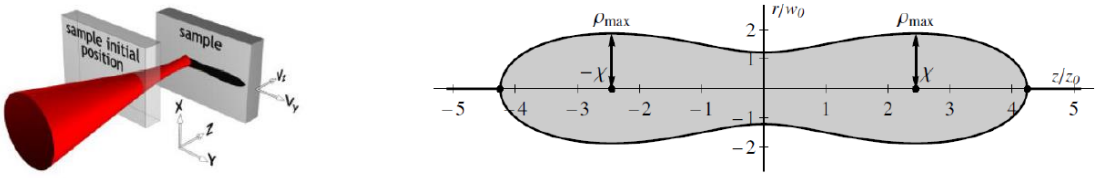

(a) (b)

Figure 1: a) D-Scan technique scheme; b) profile engraved on the surface of the sample by diagonal movement in position across the waist of the beam.

The femtosecond laser has a much shorter time width than the electron-phonon interaction time, and for this reason, a large amount of material can be ablated before most of the energy from the light beam is transferred to the crystal lattice and heat the material [6].
The use of lasers for metal machining hitherto used is based on Nd:YAG (Neodymium-doped yttrium aluminum garnet) switched lasers with time-span pulses of some tens of

nanoseconds. In this case, however, the heat produced by the interaction with the laser pulses causes a very large deformation when using very thin plates. Thus, the femtosecond laser available in the laboratories of the Lasers and Applications Center of the Nuclear and Energy Research Institute (CLA-IPEN) is an important and considerable alternative to obtain such ablated surfaces without the collateral heat production.

2. MATERIALS AND METHODS

The material chosen for this work was titanium commercially pure grade 2 (Ti Gr. 2 CP) due to its high relative strength.

2.1. Ultra-short pulse laser and beam delivery system

The system consists of a femtosecond Ti:Sapphire laser amplified by the frequency-scanning amplification method (Femtopower Compact Pro CE-Phase HP / HR of the Femtolasers brand) that continuously generates pulses of 25 fs (FWHM) centered at 775 nm with 40 nm bandwidth (FWHM), maximum repetition rate of 4 kHz and maximum energies per pulse of 750 μJ.
The drive system for the execution of the machining consists of a table with coordinated movement of the X and Y axes via the Computer Numerical Control (CNC) command, while the Z movement is manual through a micrometer. For all axes the movements have micrometric precision.
For fluency estimation, the Gaussian beam propagation model is used to calculate the theoretical value of the beam diameter on the sample surface. Thus, the theoretical beam diameter in the sample was determined according to Eq. (1) [7].

$$\Phi = \frac{4.M^2.\lambda.f}{\pi.\Phi_0} \quad (1)$$

where ϕ is the beam diameter at the focus, M^2 is the beam quality factor, λ is the laser wavelength, f is the focal length of the lens and ϕ_0 is the beam diameter at the lens input. Once the theoretical beam diameter at the sample surface is determined, the energy flow per pulse is calculated by the ratio of beam energy to beam area at the focus ($F_0 = E / Af$).

2.2. Determination of the ablation threshold by the D-Scan method

The D-Scan method was performed on a sample of Ti Gr. 2 CP with dimensions of 10 mm x 20 mm and thickness of 2.0 mm. In the method, 28 strokes were performed, with repetition rates of 100 Hz, 500 Hz and 4000 Hz, energies ranging from 67.2 μJ to 71.2 μJ, overlapping from 0.24 to 7.950.50 pulses. The inert gas argon (Ar) with a purity greater than 99.999% with a flow rate of 8.0 L/min was used to protect the atmosphere of the ablated regions.
Through the Scanning Electron Microscope (SEM), the images of each ablated profile were captured and thus measured at half the transverse dimension of each of the 28 recorded profiles, so that the F_{th} x D^2 graph could be traced.

2.3. Analysis by Scanning Electron Microscopy (SEM), X-ray Diffraction and Wettability

The SEM analyzes were done on a TM3000 microscope model Hitachi with 20x, 300x, 800x and 1000x magnification. X-ray diffraction (XRD) was performed using the Rigaku X-ray diffractometer model Multiflex at 40 kV and 20 mA using Cu-kα radiation (λ = 1.54184 Å). Sample 3 of the micro-machining 01 (F_0 = 23.2 J / cm²) and sample 3 of the micro-machining 03 (F_0 = 3.3 J / cm²) were selected for the analysis. Measurement of wettability was performed by the sessile drop contact angle method according to ASTM D 5725-99 using a HTL brand micrometer volume control pipette model LM10 and an arrangement consisting of an optical assembly with a camera CMOS brand Thorlabs model DCC1545C resolution 1280x1024 pixels, coupled to a zoom system with variable magnification up to 12 times.

3. RESULTS AND DISCUSSION

3.1. Ablation threshold by the D-Scan method

In the D-Scan method, 28 traces were recorded, whose recorded profiles can be seen in Fig. 2, as well as the graph of the flow as a function of the number of pulses (F_{th} *x N*) to determine the ablation threshold for the low and High fluency, shown in Fig. 3.

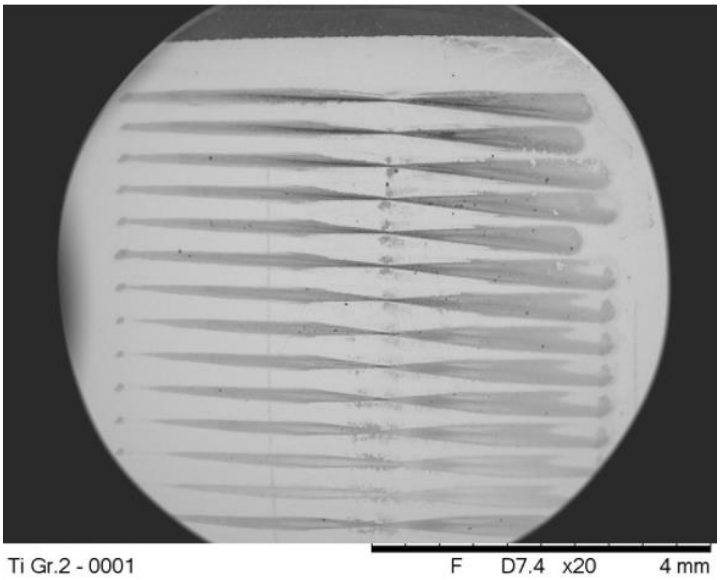

Figure 2. SEM image of the ablated traces in the Ti Gr. 2 CP sample by the D-Scan method with 20x magnification

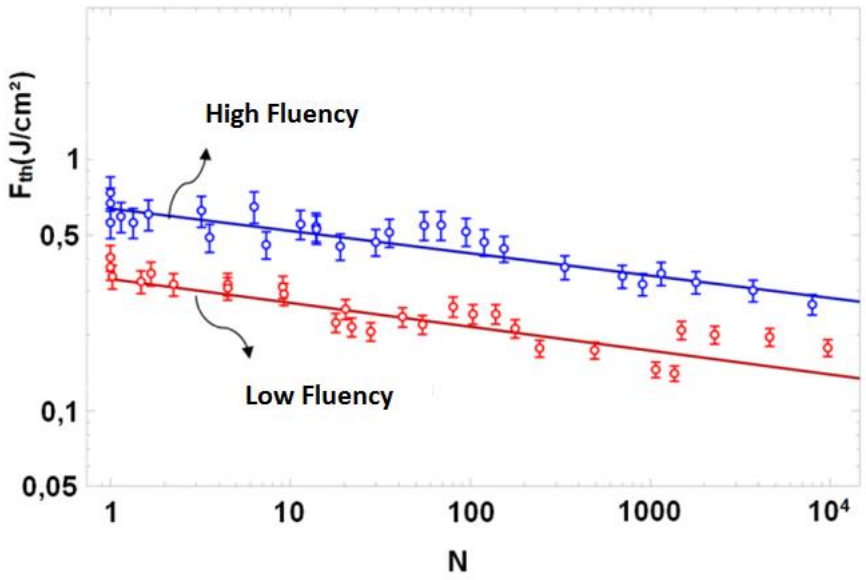

Figure 3. Graphic F_{th} as a function of the number of N superimposed pulses for the D-Scan method.

From the graph of Fig. 3 it is seen that the ablation threshold for the low fluency regime for 1 pulse is F_{th} = 0.330 ± 0.006 J / cm², and for the high fluency regime is F_{th} = 0.640 ± 0.006 J / cm².

3.2. Micro-machining of Ti Gr. 2 CP slides with 0.1 mm thickness using ultrashort pulsed laser

In the determination of the ablation threshold by the D-Scan method, the samples had a thickness of 2 mm. It was possible to observe the non-occurrence of resolidified material in the ablated regions, even in the high fluency regime. In this way, six (6) microstructures were performed on slides with a thickness of 0.1 mm, using fluency values from 0.44 ± 0.04 J/cm² (micro-machining 1), which is close to the threshold, up to 18.35 ± 0.04 J/cm² (micro-machining 6), in order to certify the absence of warpage. The overlap of pulses was 50 for the micro-machining 1 and reduced for 1,144 to the micro-machining 2, and from the micro-machining 3 to the micro-machining 6 there was no overlap, that is, the ablated points were spaced. In all cases, the inert gas argon (Ar) with a purity greater than 99.999% was used with a flow rate of 8.0 L/min to protect the atmosphere. It is worth noting that the diameter used for these calculations was the theoretical diameter of the laser beam focused on the sample according to Equation 1, which was 24 μm. For larger fluences, the damage is greater and the spacing must be larger.

In micro-machining 1, which has the greatest overlap, the incubation effect promoted the greatest reduction in the ablation threshold, being the condition where the greatest thermal input occurred. Micro-machining 1, 2 and 4 can be seen in SEM images in Fig. 4, where the overlapping of pulses for the first case and the distancing of the pulses in the others can be observed.

As the overlap is increased, the relationship between the size of the damage and the theoretical diameter of the pulse in the focus increases, which is the direct consequence of the incubation effect. It can also be noticed that in the micro-machining 2 the overlap was

minimal, that is, with an overlap of only 14.4%. Due to the combination of frequency and velocity parameters, there was no overlap in the 3, 4, 5 and 6 microwaves, thus point trails were obtained for these cases.

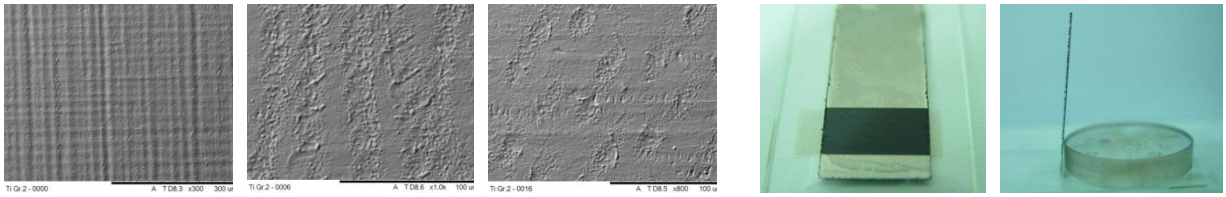

(a) (b) (c) (d) (e)

Figure 4. SEM images a) in the slide of 0.1 mm thickness of the micro-machining 1 with 300x magnification, b) of the micro-machining 2 with 1000x magnification, c) and of the micro-machining 4 with 800x magnification. Photograph d) of the blade with the micro-machining 1 top view and e) of the profile view.

Even in the extreme condition, which was the micro-machining 1, there were no deformations of the lamina, proving that even in the regime of high fluency there is no significant heat transfer to the crystalline lattice that could cause such deformations. Fig. 4 (e) shows the blade with this micro-machining, and it can be verified that there was no evidence of surface deformation causing warpage and distortion.

However, in the micro-machining where no overlapping of pulses occurred, machining of the dimples would require an extremely high time for execution. This implies that there would be a need for repeated passes in the same region for overlapping to ensure good depth at the ablated points. In this way, the realization of "dimples" by the available system would be impracticable, which directed the work to another strategy, which would be the realization of "traces in meshes" to obtain micro-machining.

As the dots matrix produced in the previous process led to very shallow damage, three micro-machinations with a higher energy flow per pulse and considerably greater overlap than the micro-machining 1 were defined, aiming the micro-machining of traces with a large overlap of pulses and the production of deep grooves. The three microstructures on the 0.1 mm thick slides were machined using the argon inert gas with a purity greater than 99.999% with a flow rate of 8.0 L/min to protect the atmosphere.

To prepare the micro-machining, it was decided to perform cross-zigzag micro-machining on the 0.1 mm blade. For the execution of these cross zig-zag geometries there was only the variation of the step between the machined lines, being 75 μm for micro-machining 01, 100 μm for micro-machining 02 and 200 μm for micro-machining 03. The energy flow per pulse was 3.32 ± 0.04 J/cm² and the overlap was 1150 pulses for the 3 (three) micro-machining.

After the execution of the microstructures, SEM analyzes were performed, the images obtained are shown in Fig. 5. Thus, it was analyzed and verified that even in this extreme condition of the zig-zag geometry, that is, a condition where a considerable removal of material with sensitive depth there was no deformation of the blade.

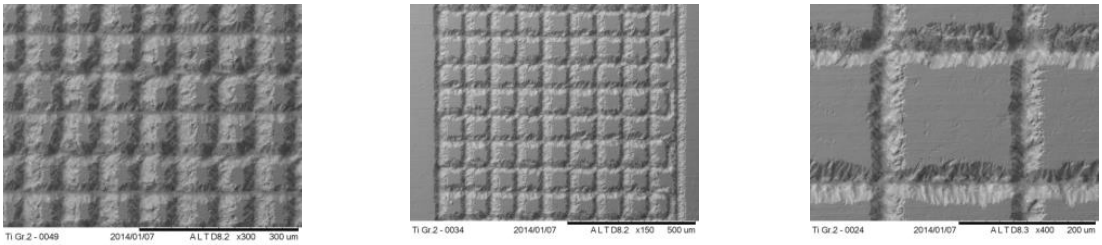

(a) (b) (c)

Figure 5. SEM images of micro-machining with cross zig-zag geometries in a 0.1 mm thick slide. a) Microsupport 01 with increase of 300x; b) micro-machining 02 with increase of 150x; and c) micro-machining 03 with a magnification of 400x.

The images of the micro-machining 01 in three dimensions obtained in the SEM are shown with the help of the software 3D-Image Viewer in Fig. 6, where it can be noticed that the 0.1 mm thick slide did not suffer deformations and warping. By the analysis of the topography it was possible to measure the depth of the micro-machined regions, which resulted in an average value of 14.50 μm.

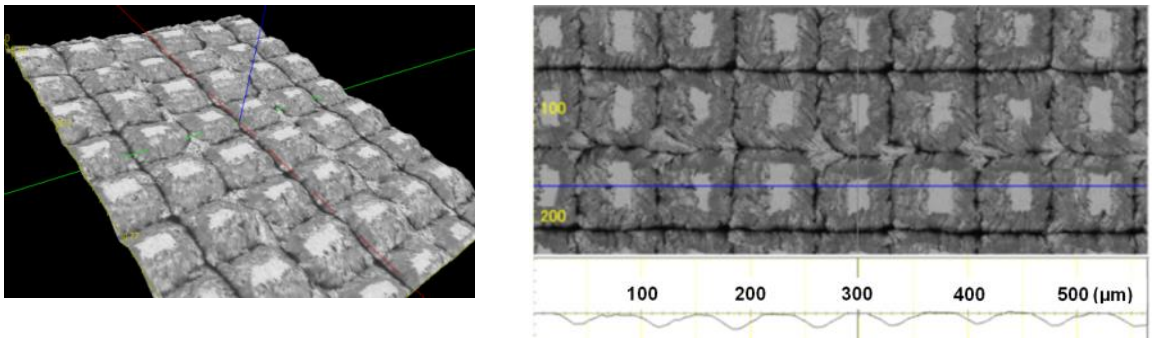

Figure 6. SEM images in three dimensions of the zigzag 01 micro-aliasing through the 3D-Image Viewer software with a 300x magnification.

The parameters used to make these micro-machinations provided a very favorable condition due to the considerable overlapping of pulses and to have promoted a satisfactory depth, besides not being evidenced the existence of resolidified material and also presented no evidence of warpage. Under these conditions, it was expected that the bonding would have a good efficiency.

Fig. 7 shows SEM image with lines made in the determination of the ablation threshold by the D-Scan method, where it is possible to see the region affected by the low fluency regime, which is the region close to the machined line. These lines were performed with energy flow per pulse and overlapping similar to the conditions in which micro-machining were performed

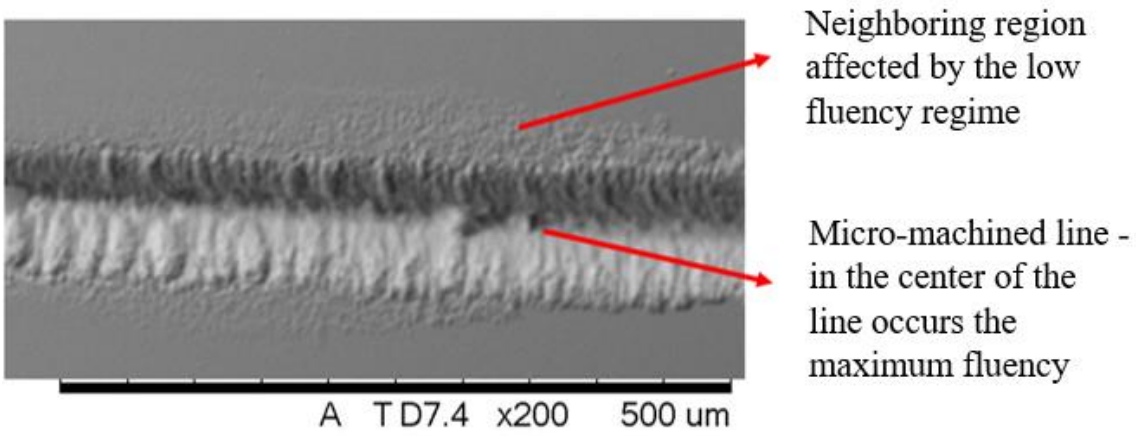

FIGURE 7. Line SEM image performed in the D-Scan method with energy flow per pulse and overlap similar to the conditions of the micro-machining. With 200x magnification.

3.3. Micro-machining in 2 mm thick samples

From the conclusion that it would be possible to operate in the high fluency regime without any deformations in the samples, 2 mm thick samples were then micro-machined. This was necessary, as it would not be possible to carry out a tensile test in the case of 0.1 mm blades. Micro-machining were performed in 3 (three) samples of the micro-machining 01, 3 (three) samples of the micro-machining 02 and 3 (three) samples of the micro-machining 03 with the same parameters of the previous case.
The sample sizes were 60 mm x 10 mm and 2 mm thick, and the micro-machined area was 10 mm x 10 mm at the end of the samples. In order to protect the atmosphere, the argon inert gas was used with a purity greater than 99.999% and a flow rate of 8.0 L/min.

3.4. X-ray diffraction (XRD) in 2.0 mm-thick micro-machined samples

For the analysis of diffraction X-ray micro-machined samples shown in Fig. 8 and Fig. 9, it was found that no β phase (cubic crystal structure of body-centered) retained since the presence of Ti was detected only only in its α phase (crystalline hexagonal structure Compact) - Powder Diffraction File PDF 05-0682. It is worth mentioning that the technique used has a sensitivity to detect in a layer of up to 1 μm, so if there was presence of β phase, it would be in a layer smaller than 1 μm. Thus, in the laser ablation process of ultrashort pulses, there was no presence of β phase after cooling.
Even though it operates in the regime of high fluency, and that caused formation of liquid phase, no resolidified material is observed. This probably occurred because the molten material was ejected out of the affected region, and did not have the time (or sufficient energy) to heat the neighboring region and cause a zone affected by detectable heat. Thus, even with high fluency, the crystalline structure of the surface is not modified and, therefore, does not generate tensions that would lead to the deformation of the part.
However, because titanium has a high affinity for oxygen, the presence of TiO in the sample can be verified with micro-machining 01 (Powder Diffraction File - PDF 89-3077) and in the sample with micro-machining 03 (Powder Diffraction File - PDF 71-5272), even with

atmosphere protection from interaction with inert gas argon. Thus, due to the extreme reactivity of titanium and oxygen, even with the use of argon, there was still the reaction with oxygen and the consequent formation of oxides. One way to avoid or minimize this reaction would be to use a glove box with very low oxygen concentration.

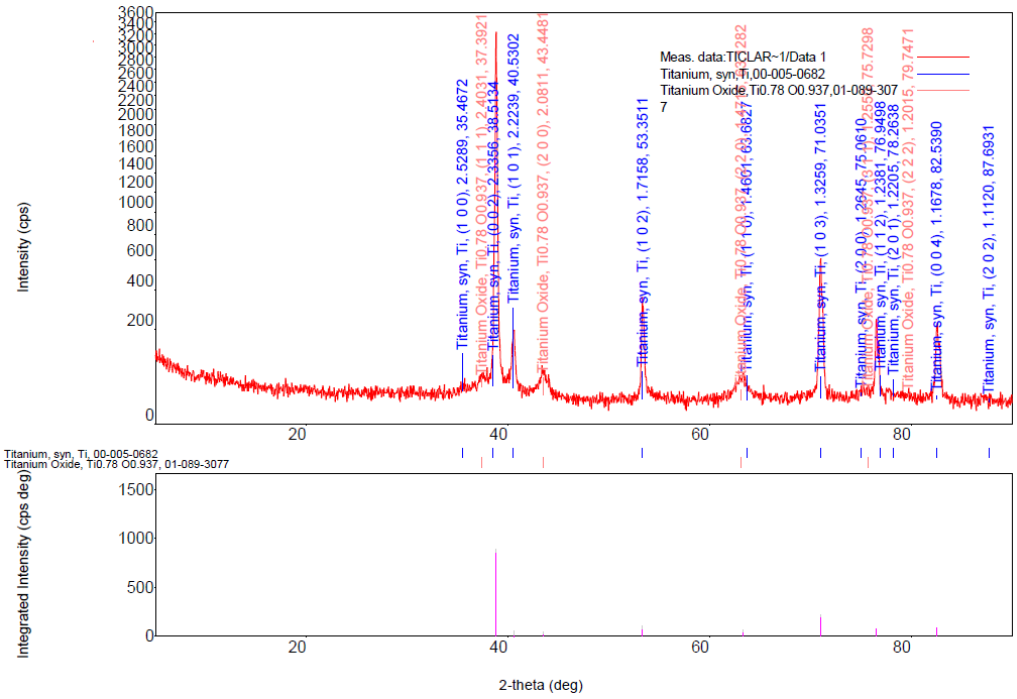

FIGURE 8. X-ray Diffractogram of sample with micro-machining 01.

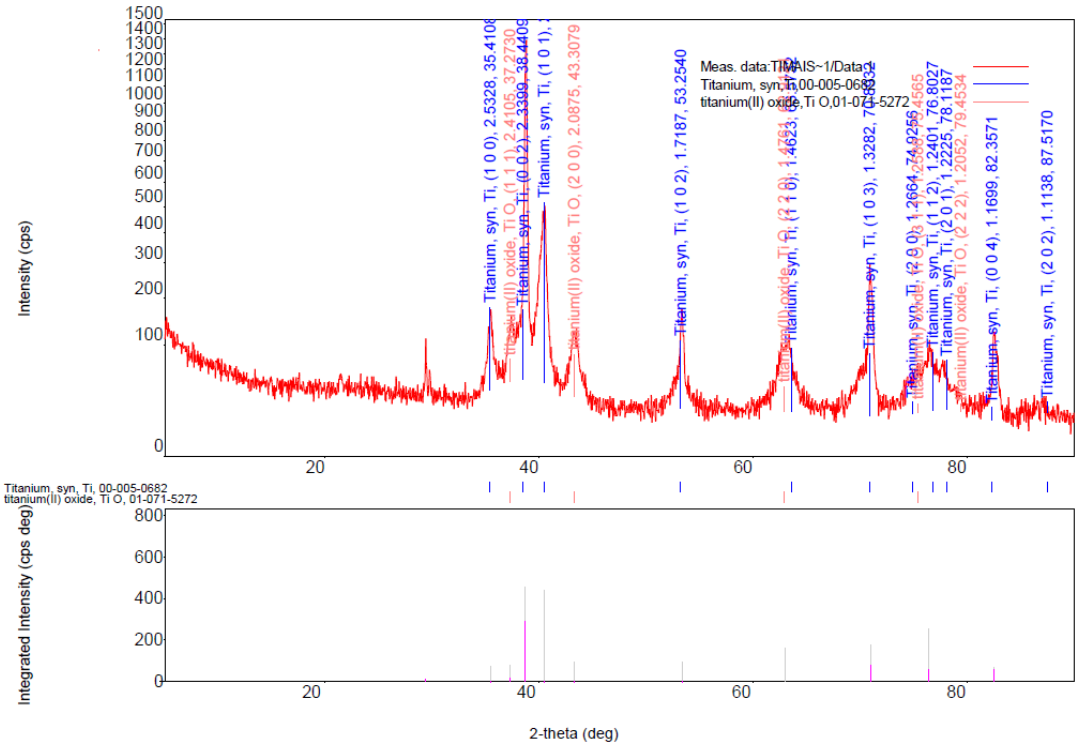

FIGURE 9. X-ray Diffractogram of sample with micro-machining 03.

3.5. Measurement of wettability

The images of the bead profiles are shown in Fig. 10, and with the aid of the ImageJ software, Fig. 11, the contact angles as shown are determined.
The measurements of the contact angles indicated the values of 99.85°, 83.56° and 50.08° for the micro-machining 01, 02 and 03 respectively, whereas for the surface without micro-machining it resulted in the value of 39,54°. The results of the wettability for each sample indicate the decrease of the contact angle with the increase of the micro-machining step, which increased surface hydrophilicity and consequently improved wettability. It can still be seen that the sample without micro-machining presents the best wettability.

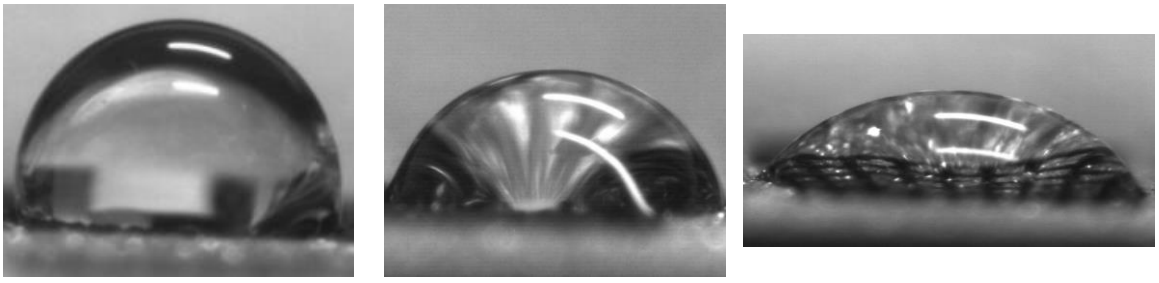

(a) (b) (c)

Figure 10. Drop profile image for measurement of wettability by the sessile drop method in a) micro-machining 01; b) micro-machining 02; and c) micro-machining 03.

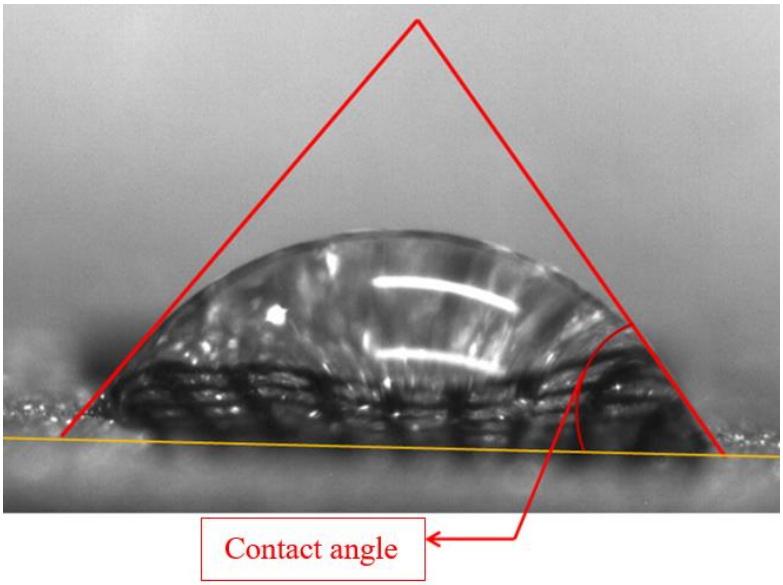

Figure 11. Image of the micro-machining 03 in the Image J software - lines represent the references for determining the contact angle of the drop.

It is important to note that in this experiment, although the method used followed the recommendations of ASTM D 5725-99, no specific equipment was used to measure wettability, and thus the values obtained may show some variation in relation to what would be found in such equipment, thus the quantitative analysis does not offer reliability as to the exact values, but allows to analyze the variations for each machined geometry. In this way the values obtained have a much more qualitative character for the purpose of comparison of each micro-machining performed than for determining the wettability characteristics of the surfaces.
The immediate effect of micro-machining of the metal surface is the influence exerted on the contact angle of the drop, modifying its surface properties.

3. CONCLUSIONS

By means of obtaining the ablation thresholds for Ti Gr. 2 CP, by ultrashort pulses of femtoseconds, the D-Scan method was able to determine the high and low fluency regimes. With the system used in this work it was not possible to obtain micro-machining of "dimples" with femtosecond laser pulses, as this would be extremely time-consuming. The alternative of working on the high fluency regime to produce a "traces in mesh" geometry proved to be efficient. Through the knowledge of the ablation thresholds, microstructures were performed in three conditions on slices of Ti Gr. 2 CP of 0.1 mm thickness. Such micro-machining was performed in the high fluency regime, since even in this condition it did not lead to distortion and warpage to the blades, besides that the melt was totally expelled out of the processed region, leaving a surface free of resolidified material. The heating time, and / or the energy input was not sufficient to produce a ZTA large enough to be detected, in addition to having promoted a satisfactory depth.
The micro-machining analysis allowed the measurement of the wettability and specific volumes for each unit cell as well as the total volume available. In this way, it was verified that the lower the wettability, the greater the number of unit cells and consequently, the greater the total volume available.

In this way, the use of ultrashort pulsed laser was extremely satisfactory for the execution of micro-machining in Ti Gr. 2 CP, with the possibility of performing micro-machining with variations in the geometries and that also allow the extension of the study to other metals, maintaining the integrity of the material and with excellent quality of the ablated region.
Finally, from the studies presented here the challenge is now to research Maraging Steels and Zircaloy. To this end, micro-machining will be performed to obtain traceability markings on the surfaces of components used in the nuclear industry in a way that does not compromise the integrity and reliability of such components. In this way, with the change of the surface with a very small removal of material it is expected that the use of ultra-short pulse lasers will provide great benefits to guarantee the integrity of the ablated material.

ACKNOWLEDGMENTS

The authors thank FAPESP (Project 2013 / 26113-6), IPEN, Technological Center of the Navy in São Paulo (CTMSP) and Sorocaba College of Engineering (FACENS) for the support and support given to the development of this research.

REFERENCES

1. R. E. Samad, L. M. Machado, N. D. Vieira Jr., W. De Rossi. “Ultrashort Laser Pulses Machining”, In: I. Peshko (Ed.) *Laser Pulses - Theory, Technology, and Applications,* InTech, pp. 143-174 (2012).
2. J. Jandeleit, A. Horn, R. Weichenhain, E. W. Kreutz, R. Poprawe. “Fundamental investigations of micromachining by nano- and picosecond laser radiation”, *Applied Surface Science*, **129**, pp. 885-891 (1998).
3. P. P. Pronko, S. K. Dutta, J. Squier, J. V. Rudd, D. Du, G. Mourou. “Machining of sub-micron holes using a femtosecond laser at 800 nm”, *Optics Communications*, **114 (1)**, pp. 106-110 (1995).
4. N. M. Bulgakova, R. Stoian, A. Rosenfeld, I. V. Hertel, E. E. B. Campbell. “Electronic transport and consequences for material removal in ultrafast pulsed laser ablation of materials”, *Physical Review B- Condensed Matter and Materials Physics*, **69 (5)** 054102, pp. 1-12 (2004).
5. D. Ashkenasi, A. Rosenfeld, R. Stoian. “Laser-induced incubation in transparent materials and possible consequences for surface and bulk micro-structuring with ultra short pulse”, *Society of Photo-Optical Instrumentation Engineers (SPIE)*, **4633** (**1)**, pp. 90-98 (2002).
6. R. E. Samad, N. D. Vieira Jr. “Geometrical method for determining the surface damage threshold for femtosecond laser pulses”, *Laser Physics*, **16 (2)**, pp. 336-339 (2006).
7. A. E. Siegman. *Lasers*. University Science Books, Salsalito, CA, United States (1978).